Cell, Vol. 105, 711–720, June 15, 2001, Copyright ©2001 by Cell Press

# Molecular Insights into Polyubiquitin Chain Assembly: Crystal Structure of the Mms2/Ubc13 Heterodimer

**Andrew P. VanDemark,[1] Roseanne M. Hofmann,[2,5] Colleen Tsui,[2] Cecile M. Pickart,[2] and Cynthia Wolberger[1,3,4]**

[1] Department of Biophysics and Biophysical Chemistry
School of Medicine
[2] Department of Biochemistry
School of Public Health
[3] Howard Hughes Medical Institute
Johns Hopkins University
Baltimore, Maryland 21205

## Summary

**While the signaling properties of ubiquitin depend on the topology of polyubiquitin chains, little is known concerning the molecular basis of specificity in chain assembly and recognition. UEV/Ubc complexes have been implicated in the assembly of Lys63-linked polyubiquitin chains that act as a novel signal in postreplicative DNA repair and IκBα kinase activation. The crystal structure of the Mms2/Ubc13 heterodimer shows the active site of Ubc13 at the intersection of two channels that are potential binding sites for the two substrate ubiquitins. Mutations that destabilize the heterodimer interface confer a marked UV sensitivity, providing direct evidence that the intact heterodimer is necessary for DNA repair. Selective mutations in the channels suggest a molecular model for specificity in the assembly of Lys63-linked polyubiquitin signals.**

## Introduction

Protein modification by ubiquitin serves a signaling function in diverse biological processes, including cell cycle progression (Koepp et al., 1999), oncogenesis (Joazeiro and Weissman, 2000; Joazeiro et al., 1999), and antigen presentation (Rock and Goldberg, 1999). The ability of ubiquitin to signal substrate proteolysis by the 26S proteasome underlies many of ubiquitin's cellular functions (Hershko and Ciechanover, 1998). However, ubiquitin also serves as a nonproteolytic signal in DNA repair (Jentsch et al., 1987; Spence et al., 1995) and IκBα kinase (IKK) activation (Chen et al., 1996). Ubiquitin conjugation also serves a signaling function in endocytosis that leads to proteolysis in the lysosome/vacuole (Hicke, 1999), and ubiquitin conjugation can modulate the structural organization of multiprotein assemblies (Kaiser et al., 2000).

The biologically active ubiquitin signal frequently consists of a polyubiquitin chain in which successive ubiquitins are joined through isopeptide bonds involving specific lysine residues of ubiquitin. In some cases, the fate of a ubiquitin-conjugated protein can be correlated with the chemical structure of the polyubiquitin chain (Chau et al., 1989; Deng et al., 2000; Finley et al., 1994; Hofmann and Pickart, 1999; Koegl et al., 1999; Pickart, 2000; Spence et al., 1995). For example, polyubiquitin chains linked through Lys48 (K48-chains) are the principal signal for proteolysis by 26S proteasomes (Chau et al., 1989; Finley et al., 1994), whereas Lys63-linked chains (K63-chains) are required for postreplicative DNA repair (Hofmann and Pickart, 1999; Spence et al., 1995), IKK activation (Deng et al., 2000), translational regulation (Spence et al., 2000), and certain cases of ubiquitin-dependent endocytosis (Galan and Haguenauer-Tsapis, 1997). Blocking K63-chain assembly has no effect on proteasomal degradation in vivo (Spence et al., 1995), and IKK activation can be reconstituted in vitro in the definitive absence of proteasomes (Deng et al., 2000). IKK activation is selectively inhibited by free K63-chains, and not K48-chains (Deng et al., 2000). Thus, while the precise signaling functions of K63-chains remain to be defined, it is highly unlikely that these chains signal proteolysis by proteasomes.

The ubiquitination of a protein substrate involves the formation of an isopeptide bond between a substrate lysine residue and the C-terminal carboxyl group of ubiquitin Gly76. This reaction is accomplished through the sequential actions of three enzymes: a ubiquitin-activating enzyme (E1), a ubiquitin-conjugating enzyme (E2 or Ubc), and a ubiquitin-protein ligase (E3) (Hershko and Ciechanover, 1998). E1 forms an initial thioester bond with the carboxyl terminus of ubiquitin in an ATP-dependent reaction. Ubiquitin is then transferred to the active site cysteine of the E2. Isopeptide bond formation results from attack on the E2 bound ubiquitin by a lysine residue of the substrate. This final reaction usually requires the participation of an E3 that binds both the E2 ubiquitin thioester and the protein targeted for ubiquitination (Hershko and Ciechanover, 1998). Lysine residues within ubiquitin may also serve as substrates, leading to the formation of diubiquitin and, eventually, polyubiquitin chains. While the overall folds of monomeric E2 enzymes, both alone and in complex with E3 ligases, have been determined (Cook et al., 1992; Huang et al., 1999; Jiang and Basavappa, 1999; Worthylake et al., 1998; Zheng et al., 2000), a plausible molecular mechanism for catalysis or specificity in ubiquitin-substrate conjugation has not yet emerged. Furthermore, the key question of how polyubiquitin chains are selectively linked through specific lysine residues has not previously been addressed.

Ubiquitin E2 variant (UEV) proteins play a central role in the assembly of K63-linked polyubiquitin chains (Deng et al., 2000; Hofmann and Pickart, 1999; Sancho et al., 1998; Ulrich and Jentsch, 2000). UEVs are similar in sequence to E2s, but lack the active site cysteine residue, indicating that UEVs must serve a fundamentally different role in ubiquitin conjugation from that performed by canonical E2s (Broomfield et al., 1998; Sancho et al., 1998). The UEVs characterized to date function together with a canonical E2, Ubc13, in the assembly of K63-chains (Deng et al., 2000; Hofmann

[4] Correspondence: cwolberg@jhmi.edu
[5] Present address: Laboratory of Synthetic Protein Chemistry, The Rockefeller University, New York, New York 10021.

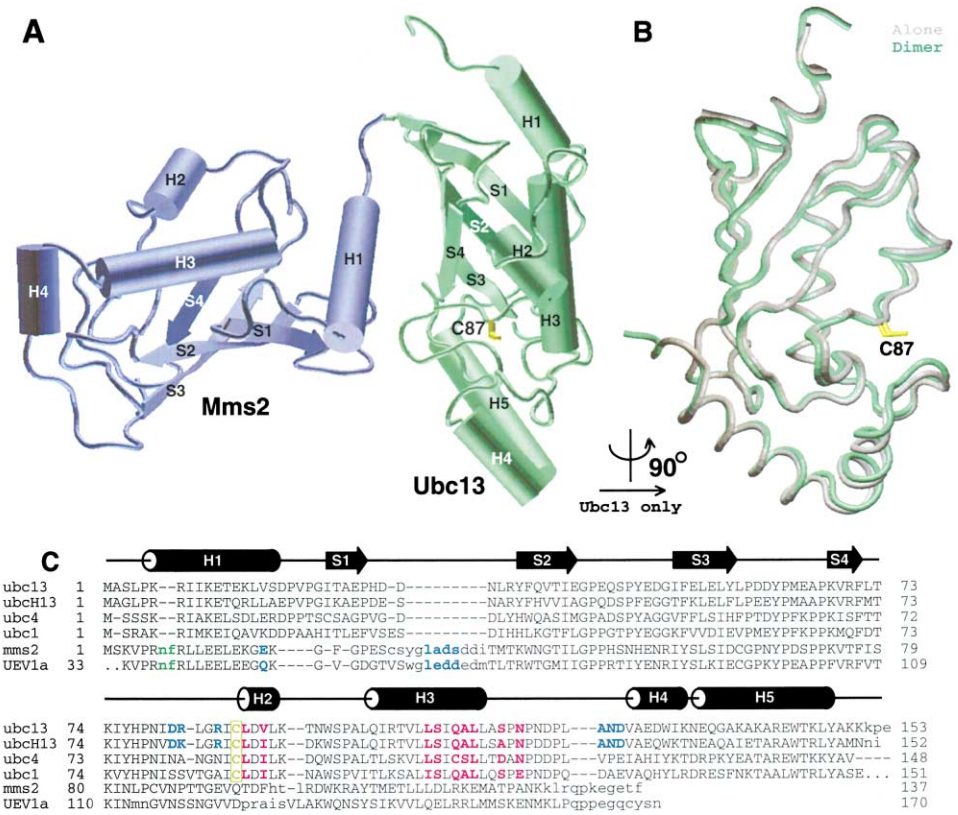


Figure 1. Structure of the Mms2/Ubc13 Complex

(A) Cartoon representation of Mms2/Ubc13 complex with Mms2 in blue and Ubc13 in green. Helices and strands are labeled. The side chain of the active site residue Ubc13-Cys87 is shown in yellow.

(B) Alignment of Ubc13 from complex, green, with Ubc13 alone structure, gray. Only Cα are shown, plus Ubc13-Cys87 for orientation.

(C) Primary sequence alignment of selected E2s and UEVs. The E2 active site cysteine position is outlined by a tan box; the Mms2 insertion containing F8 is shown in green. Ubc13 surface residues that are part of channel 1 are shown in magenta. Residues of UEVs and Ubc13s that make up channel 2 are shown in blue. Alignment was done with DALIGN.

and Pickart, 1999). The yeast UEV protein, Mms2, is required together with Ubc13 for *RAD6*/*RAD18*-dependent postreplicative DNA repair in yeast (Broomfield et al., 1998; Hofmann and Pickart, 1999). In vitro, Mms2 and Ubc13 form a complex that catalyzes the assembly of K63-chains, which function as a specific signal in the DNA repair pathway (Hofmann and Pickart, 1999; Spence et al., 1995). A related human UEV1a/Ubc13 heterodimer synthesizes K63-chains that are required for IKK activation (Deng et al., 2000). Both the yeast and human heterodimers interact with a RING domain protein that may be either a cognate E3 or a substrate of the respective E2/UEV heterodimers (Deng et al., 2000; Ulrich and Jentsch, 2000).

Although UEV proteins were initially thought to be catalytically inert (Broomfield et al., 1998; Koonin and Abagyan, 1997; Sancho et al., 1998), the Mms2/Ubc13 and UEV1a/Ubc13 heterodimers catalyze the assembly of K63-chains in the absence of any other factor besides E1 (Deng et al., 2000; Hofmann and Pickart, 1999). Chain assembly is absolutely dependent on the presence of Mms2 or UEV1a in the respective heterodimers, but the role played by the UEV subunit in catalysis and specificity has not been understood. Here we report the 1.6 Å resolution structure of the Mms2/Ubc13 heterodimer, whose architecture is likely to be conserved among the known UEV/E2 complexes. We present mutagenesis experiments that demonstrate the importance of the quaternary arrangement of the heterodimer for in vitro enzymatic activity and in vivo DNA repair, and identify residues that participate in binding the two ubiquitin proteins that become linked during conjugation. Based on our structural results and the catalytic properties of the mutant enzymes, we propose a model for molecular specificity in the assembly of K63-linked polyubiquitin chains.

## Results and Discussion

### Overall Structure of the Mms2/Ubc13 Heterodimer

Mms2 and Ubc13 form a T-shaped dimer that arises from asymmetric interactions between the two E2-like monomers (Figure 1A). Ubc13 displays the canonical α/β E2 fold, with a root-mean-square deviation (rmsd) in Cα positions of 1.6 Å, when compared with Ubc4 (Cook et al., 1993). The active site cysteine residue (C87) is contained in a long loop near the short helix 2 that follows β strand 4 (Figures 1A and 1C). Mms2, the UEV protein, adopts a fold similar to Ubc13 and other E2 enzymes, but with several notable differences. The seven

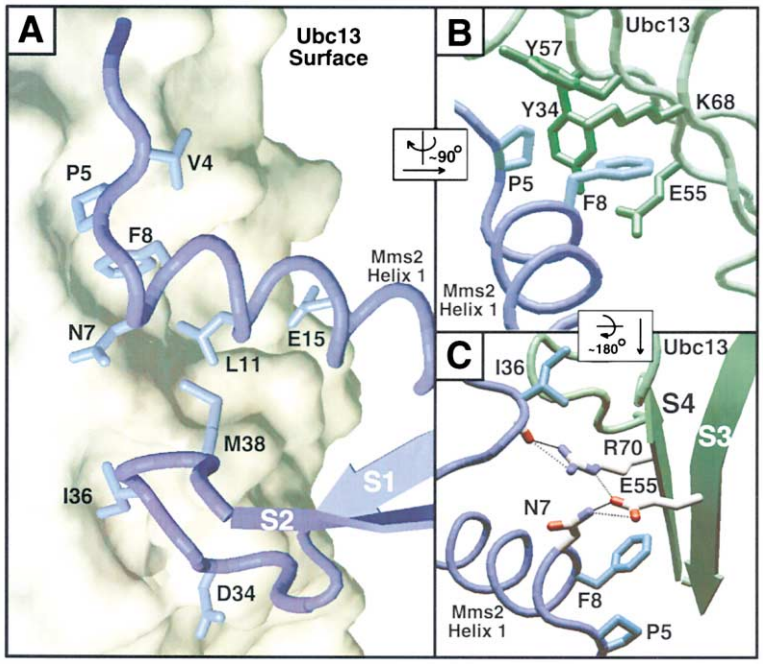


Figure 2. The Mms2/Ubc13 Binding Interface Contains Both Hydrophobic and Polar Surfaces

(A) Mms2/Ubc13 heterodimerization interface. Ubc13 is displayed as a surface with Mms2 interface residues in light blue.

(B) F8A-Mms2 (light blue) environment showing hydrophobic contacts with Ubc13 residues E55, L56, Y57, and R70 (green). The Ubc13 backbone is shown in green.

(C) E55-Ubc13 environment highlighting hydrogen bonds that bridge the interface (black). The Mms2 backbone shown in blue, the Ubc13 backbone in green.

amino-terminal residues of Mms2, which participate in complex formation with Ubc13, adopt a conformation that is atypical of E2s. This conformation allows the N terminus to participate in the dimer interface (Figure 1A). In addition, Mms2 is 16 residues shorter than Ubc13, and Mms2 residues C-terminal to helix 3 do not adopt the E2 fold. The vestigial active site loop of Mms2 (residues surrounding Mms2-Gln94) is ~44 Å away from the Ubc13 active site loop and is unlikely to function in catalysis (Figure 1A, see below).

### The Mms2/Ubc13 Binding Interface

The asymmetric interface of the Mms2/Ubc13 heterodimer is formed by packing of Mms2 helix 1 against Ubc13 β strands S3 and S4 (Figure 2A). In addition, loop residues 30–38 from Mms2 interact with Ubc13 residues 72–83 (Figure 2A) located in S4 and in the loop leading to helix 2. The interface, which is stabilized by both van der Waals and hydrogen bonding interactions, buries a total surface area of 1,435 Å$^2$. A particularly striking feature is the insertion of Phe8 of Mms2 into a hydrophobic pocket formed by residues Tyr57, Leu56, Glu55, and Arg70 of Ubc13 (Figure 2B). Phe8 is located in an insertion that is unique to UEVs (Figure 1C, green). Leu83 of Ubc13 also participates in hydrophobic contacts with Mms2 residues Leu14, Leu30, Asp34, Ile36, and Met38. Prominent hydrogen bonds are formed within the interface between Ubc13-Glu55 and Mms2-Asn7, as well as between Ubc13-Arg70 and the carbonyl group of Mms2-Ile36 (Figure 2C).

Point mutations were introduced at the Mms2/Ubc13 interface in order to verify the importance of the contacts seen in the crystal structure for heterodimerization in vitro. Alanine was substituted for residue Phe8 of Mms2, both because it is a key residue mediating binding to Ubc13 and because it is found in the two-residue insertion unique to UEVs (above). Titrating the Mms2-F8A mutant against Ubc13 showed that it had a 50- to 100-fold reduced affinity for wild-type Ubc13 as measured by the ability to catalyze the formation of K63-linked diubiquitin (Figure 3A), while direct binding assays revealed no detectable binding (Figure 3B). The Ubc13-E55A mutation also strongly reduces the affinity of Ubc13 for wild-type Mms2 (Figure 3B). Neither mutation affects Ubc13 ubiquitin thioester formation (data not shown), demonstrating that the decrease in chain synthesis (Figure 3A and data not shown) is not due to diminished recognition of the E2 active site by E1. The biochemical properties of these mutant proteins indicate that the targeted residues make important contributions to complex stability.

Deletion of the *MMS2* or *UBC13* gene inactivates the error-free branch of the yeast *RAD6/RAD18* DNA repair pathway and sensitizes cells to DNA-damaging agents such as UV light (Broomfield et al., 1998; Brusky et al., 2000; Hofmann and Pickart, 1999; Xiao et al., 2000) (solid versus dashed line, Figure 3C). To test the biological consequences of disrupting the heterodimer interface, we examined the effect of expressing Mms2-F8A together with wild-type Ubc13, or Ubc13-E55A together with wild-type Mms2, in yeast strains lacking endogenous copies of both genes. Each mutant protein, when coexpressed with its wild-type partner, confers a DNA repair defect that is essentially identical to that of the starting double null strain (Figure 3C, compare open circles and squares to inverted triangles). A similar result is obtained when the two mutant proteins are coexpressed (upright triangles, Figure 3C). The failure of the mutant proteins to support repair was not due to poor expression, as shown by Western blot analysis (Figure 3D). These results verify the importance of Mms2-Phe8 and Ubc13-Glu55 for complex stabilization and provide direct evidence that the Mms2/Ubc13 *complex*, and not just its individual constituents, is required for DNA repair.

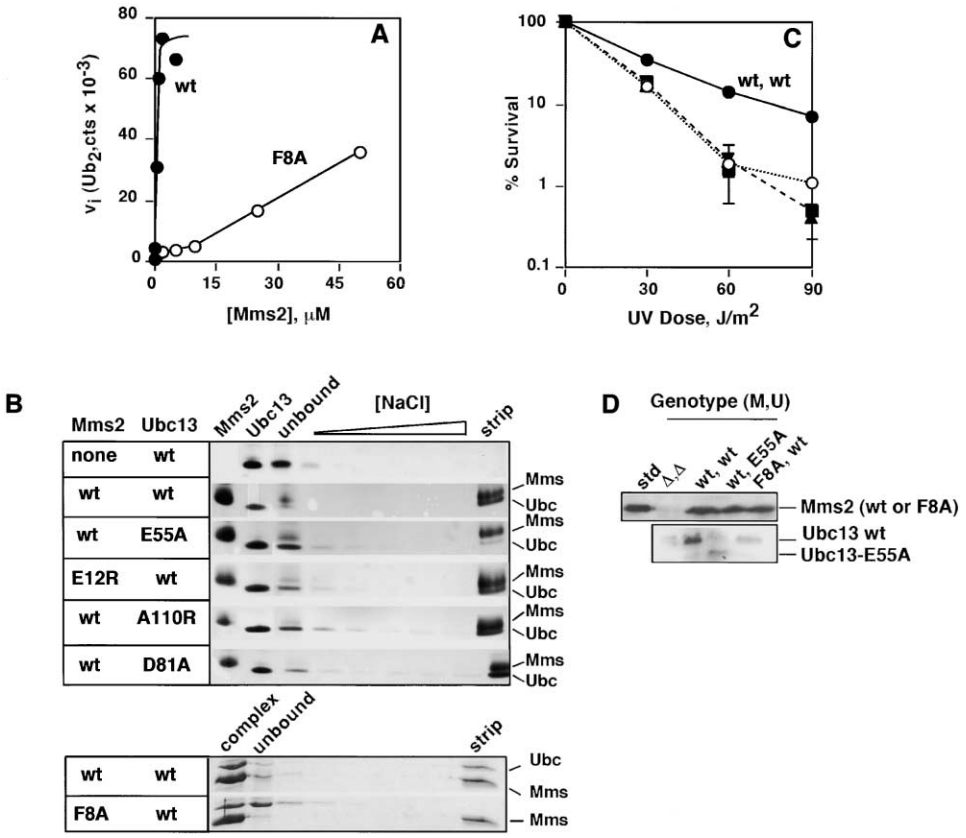


Figure 3. Biochemical Properties of Mms2/Ubc13 Interface Mutants

(A) Purified wild-type Mms2 (filled circles) or Mms2-F8A (open circles) was titrated against Ubc13 (0.5 μM) in 10 min assays of $^{125}$I-diubiquitin synthesis (Experimental Procedures).

(B) Direct binding assays. A slight excess of Ubc13 was mixed with $His_{10}$-Mms2 prior to incubation with nickel beads and elution with increasing salt concentration (50 mM to 1 M NaCl). The resin was stripped with EDTA at the end. In the bottom two strips, a slight excess of Mms2 was used; the reversed mobilities of Mms2 and Ubc13 are due to the use of different SDS-PAGE systems.

(C) Intact complex interface is required for biological activity. $His_{10}$-Mms2 and Ubc13-$HA_3$ (wild-type or mutant proteins as indicated) were expressed from separate centromeric plasmids under the control of the respective endogenous promoters in strain SUB62 (Finley et al., 1994) deleted for both endogenous genes. The tagged wild-type proteins are fully functional based on protection against UV light (R.H. and C.P., unpublished data). Inverted triangles, cells transformed with the two empty vectors; filled circles, wild-type (wt) Mms2 plus wt Ubc13; open circles, wt Mms2 plus E55A-Ubc13; squares, F8A-Mms2 plus wt Ubc13; triangles, F8A-Mms2 plus E55A-Ubc13.

(D) Expression of interface mutants in yeast cells. Selected liquid culture aliquots were lysed and extracts were probed by Western blotting for expression of $H_{10}$Mms2 and Ubc13-$HA_3$. "Std," purified $H_{10}$Mms2 protein. Purified E55A-Ubc13 migrates aberrantly in this SDS-PAGE system (data not shown).

**Interactions between Mms2/Ubc13 and Ubiquitin**

Ubiquitin polymerization by the Mms2/Ubc13 complex requires the positioning of two ubiquitin molecules in an orientation that allows Lys63 of one molecule (the acceptor) to react with Gly76 of the other (donor) molecule bound to Ubc13-Cys87. Examination of the heterodimer surface surrounding Ubc13-Cys87 reveals three distinct channels (Figure 4, green) that lead toward the active site cysteine (yellow). The channels are concave near Ubc13-Cys87 and become shallower distal to the active site (Figure 4). Channel 1 lies solely on the surface of Ubc13, while channels 2 and 3 are formed by residues from both proteins. The surface of channel 1 is hydrophobic, with a small acidic region near the active site. Channel 2 is also mainly hydrophobic, while channel 3 contains many charged residues, both basic and acidic. To test the importance of these channels in K63-chain formation, we introduced mutations designed to alter the surface properties of each channel without impeding heterodimer formation (Figure 4, blue). We then tested the mutant proteins for their ability to catalyze the formation of K63-diubiquitin in the presence of E1 and the relevant wild-type partner protein. The channel 2 mutation, Ubc13-D81A, significantly impaired chain assembly (Figure 5A), while remaining fully competent for heterodimerization (Figure 3B) and thioester formation (data not shown). Substitution of arginine at this position (Ubc13-D81R) has an even more dramatic effect, abolishing chain assembly completely (Figure 5A) without affecting E2-ubiquitin thioester formation (data not shown).

The channel 1 mutation, Ubc13-A110R, significantly inhibits chain assembly as assayed with wild-type Mms2 (Figure 5A), without inhibiting thioester bond formation (data not shown). Instead, inhibition of chain assembly reflects a 4-fold reduction in the chemical rate of isopep-

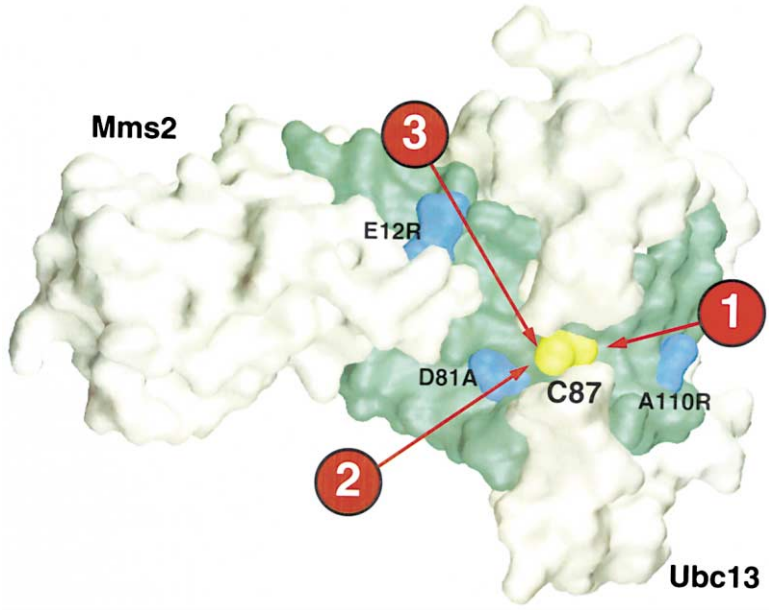


Figure 4. Channels and Interfering Mutations

The heterodimer is shown as a surface. The three channels referred to in the text are colored green and numbered, interfering mutations are shown in blue. Ubc13-Cys87 is shown in yellow. The figure was generated with VMD (Humphrey et al., 1996) and RENDER (Merritt and Bacon, 1997).

tide bond formation (as determined in a pulse-chase experiment, data not shown). These results are most simply explained if the A110R mutation interferes with the positioning of the covalently bound donor ubiquitin in channel 1 so that it is less favorably oriented for attack by Lys63 of the acceptor ubiquitin. The channel 3 mutation, Mms2-E12R, had no effect on heterodimer formation with wild-type Ubc13 (Figure 3B) or on steady-state chain assembly (Figure 5A). The complexes carrying mutations in channels 1 or 3 display $K_m$ values for the acceptor ubiquitin that are indistinguishable from that of the wild-type complex, suggesting that these

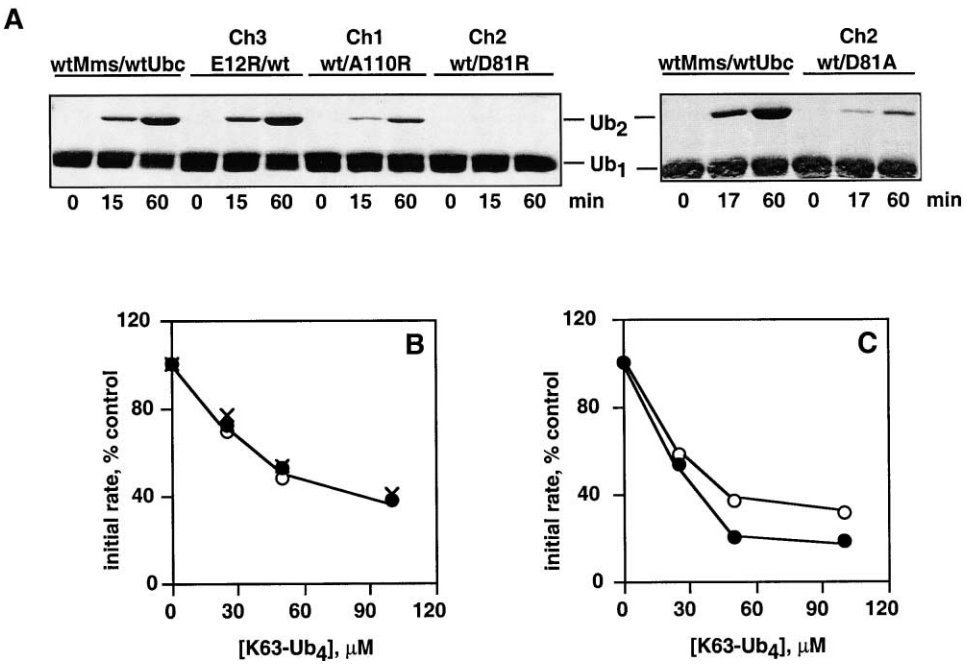


Figure 5. Biochemical Properties of Channel Mutants

(A) Diubiquitin assembly assay. D77-ubiquitin and K63R-ubiquitin (117 μM each) served as acceptor and donor, respectively, in incubations containing 2 μM Mms2/Ubc13 and 0.1 μM E1. (Coomassie-stained gel.)

(B) Binding of inert K63-tetraubiquitin to channel 1 and 3 mutants (filled circles, wild-type Mms2 plus wild-type Ubc13; crosses, wild-type Mms2 plus Ubc13-A110R; open circles, Mms2-E12R plus wild-type Ubc13). Competition was measured in assays of $^{125}$I-diubiquitin formation as described in Experimental Procedures.

(C) Binding of inert K63-tetraubiquitin to channel 2 mutant (filled circles, wild-type Mms2 plus wild-type Ubc13; open circles, wild-type Mms2 plus Ubc13-D81A).

mutations do not impede acceptor binding (data not shown). To analyze acceptor ubiquitin binding more rigorously, we used wild-type Mms2/Ubc13 complex to assemble K63-tetraubiquitin that was constrained to bind to the acceptor site, but is chemically inert. Specifically, we prevented thioester formation by placing an extra residue (D77) at the chain's proximal terminus, and blocked isopeptide bond formation by mutating the distal Lys63 to arginine (Piotrowski et al., 1997). In assays with wild-type Mms2/Ubc13 heterodimer, the purified tetramer competed effectively with a monomeric acceptor, ubiquitin-D77 (filled circles, Figures 5B and 5C). Competition by the tetramer was unaffected by the channel 1 (A110R-Ubc13) or channel 3 (E12R-Mms2) mutations (crosses and open circles, Figure 5B). These results demonstrate that neither channel 1 nor channel 3 serves as a binding site for the acceptor ubiquitin. In contrast, the Ubc13-D81A mutation in channel 2 led to diminished competition by the ubiquitin tetramer (Figure 5C), consistent with channel 2 serving as the site for acceptor ubiquitin binding.

The results of our studies suggest that channel 1, which is composed entirely of Ubc13 residues, defines the binding site for the donor ubiquitin. The proposed role for this channel is consistent with the requirement that all E2 enzymes bind a donor ubiquitin and with the high degree of sequence conservation among E2s in residues that line channel 1 (Figure 1C, magenta). Further support comes from NMR studies of a Ubc2b-ubiquitin oxyester adduct that demonstrated an interaction between this E2 and ubiquitin in the region of channel 1 (Miura et al., 1999). Our evidence supports a role for channel 2 in acceptor ubiquitin binding, as the Ubc13-D81A mutation has a dramatic affect on diubiquitin synthesis without affecting heterodimerization (Figure 3B) or thioester bond formation. The proposed role in acceptor ubiquitin binding is supported by the effect of the D81A mutation in acceptor site-specific competition assays (Figure 5C). Furthermore, the 9.2 Å distance between the active site Cys87 and Ubc13-Asp81 make it highly unlikely that this channel 2 residue is directly involved in catalysis. Residues from Ubc13 that fall within channel 2 are conserved between yeast and human Ubc13 (both of which form a UEV/E2 complex), but are not well conserved in other E2s that do not catalyze the formation of K63-linked polyubiquitin chains (Figure 1C, blue), consistent with the proposed role of these residues in acceptor ubiquitin binding.

To examine possible conformational changes within Ubc13 that might occur as a result of Mms2 binding, we determined the structure of Ubc13 alone. The 2.0 Å structure is very similar to that of Ubc13 in the heterodimer, with an rmsd of 0.8 Å for Cα atoms. An alignment of Ubc13 alone and Ubc13 from the heterodimer (Figure 1B) demonstrates the similarity, and shows that complex formation is unlikely to affect donor ubiquitin binding to channel 1. Additionally, there are no appreciable differences in the orientation of residues proximal to Cys87 in the two structures. A similar lack of E2 conformational perturbation was reported in the structures of UbcH7 with two different cognate E3s (Huang et al., 1999; Zheng et al., 2000).

### Model for Lysine63-Linked Polyubiquitin Chain Assembly

Based on the structural and biochemical data presented here, we have constructed a model for the K63-chain assembly reaction performed by the Mms2/Ubc13 complex (Figure 6). Two ubiquitins were manually docked onto the Mms2/Ubc13 structure, placing a donor ubiquitin in channel 1 and an acceptor ubiquitin in channel 2 (Figure 6, purple). The donor ubiquitin was positioned to place the Gly76 carbonyl group within 3 Å of the active site Cys87, while maximizing the shape complementarity of ubiquitin to channel 1 and minimizing steric clashes. Ubiquitin with an I44A substitution is specifically defective in binding to the acceptor (versus donor) site, suggesting that Ile44 may be located on the surface of ubiquitin that contacts the acceptor site (A. Raguraj and C.P., unpublished results). We therefore positioned the acceptor ubiquitin by requiring that ubiquitin Lys63 approach Ubc13-Cys87 via channel 2 and that ubiquitin Ile44 contact the heterodimer surface. We further required that the ε-amino group of Lys63 be within 3 Å of the Ubc13-Cys87 thiol (Figure 6)—a distance that positions the lysine side chain for nucleophilic attack on the carbonyl group of the thioester bond. In the resulting model, Ile44 of the acceptor ubiquitin contacts Mms2 in the region of Ile57 (Figure 6). Shape constraints alone were taken into account during manual model building.

A similar model was arrived at using the automated docking program, 3-D Dock (Gabb et al., 1997), which takes both electrostatics and steric constraints into account. The program was used to produce a set of solutions for the docking of a single ubiquitin monomer on the surface of the Mms2/Ubc13 heterodimer. When no constraints are imposed on the docking program, the highest-ranking solutions have the ubiquitin docked into either the donor site that lies on Ubc13 (channel 1), or on the corresponding surface of Mms2 near the vestigial active site. The latter set of solutions, however, does not place Lys63 (or any other lysine) of the docked ubiquitin sufficiently close to the enzyme active site to be a plausible model for acceptor ubiquitin binding. In order to identify other possible docking solutions that could represent the binding of acceptor ubiquitin, the results of the unconstrained search were sorted to eliminate solutions that failed to place Lys63 of ubiquitin within 4.5 Å of the active site cysteine, Ubc13-Cys87. The remaining solutions contain a ubiquitin docked into the acceptor site in essentially the same orientation as that obtained by the manual docking procedure. Interestingly, neither manual nor computational approaches to positioning an acceptor ubiquitin with Lys48 near the active site cysteine yielded a plausible model, consistent with the proposed role of channel 2 of the heterodimer in orienting ubiquitin for K63-linked chain formation.

The model presented here provides a straightforward explanation for linkage specificity in polyubiquitin chain assembly. As is the case for other E2 enzymes, Ubc13 acts as a donor that transfers a covalently bound ubiquitin to a lysine residue on an acceptor protein. Mms2, the catalytically inactive E2-like protein, binds to Ubc13 and thereby forms an acceptor ubiquitin binding channel at a junction between the two proteins. The residues that line the acceptor channel orient the bound ubiquitin so that the Ubc13 bound donor ubiquitin is transferred

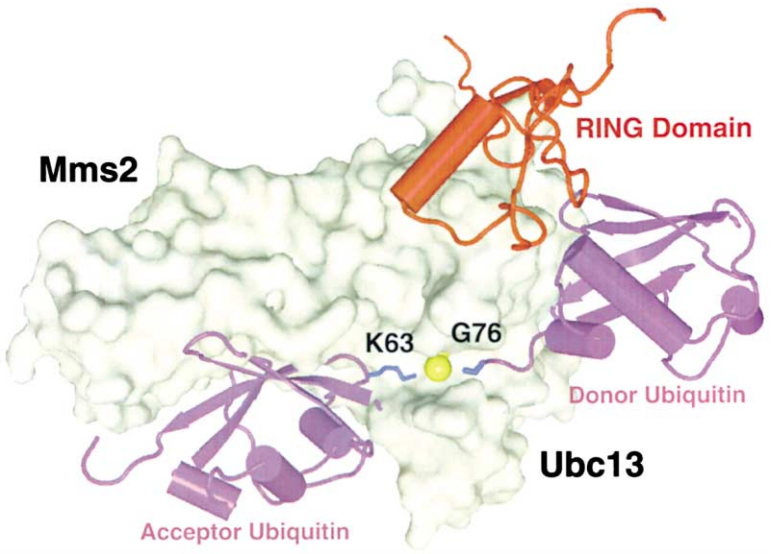


Figure 6. Model for Interaction of Mms2/Ubc13 Complex (Surface) with Rad5 (Red) and Two Ubiquitin Proteins (Purple)

The donor Ub and acceptor Ub were positioned to place the C termini of the donor Ub and K63 of the acceptor Ub within 3 Å of the active site thiol (yellow) while avoiding steric clashes. Other modeling criteria are described in the text. The acceptor ubiquitin is at the lower left; the donor ubiquitin is at the right.

specifically to Lys63 of the acceptor ubiquitin. This model predicts that the use of different lysine residues in chain assembly will be associated with interactions between distinct ubiquitin surfaces and specific chain-assembling enzymes/complexes. Consistent with this idea, the I44A mutation in ubiquitin, which blocks binding to the Mms2/Ubc13 acceptor site, is permissive for the assembly of K48-chains by two different enzymatic pathways (Beal et al., 1996).

### Proposed RING-Heterodimer Interactions

The Mms2/Ubc13 complex has been shown to interact with the Rad5 helicase, a component of the *RAD6/RAD18* pathway that also features a zinc binding RING domain (Brusky et al., 2000; Johnson et al., 1992; Ulrich and Jentsch, 2000). Rad5 associates with the heterodimer via a direct interaction with Ubc13 (Ulrich and Jentsch, 2000). Many E3 enzymes, including the protooncogene c-Cbl, contain RING domains (Joazeiro and Weissman, 2000). The c-Cbl/UbcH7 cocrystal structure revealed that the E2 (UbcH7) binds the RING domain of c-Cbl by inserting phenylalanine and proline side chains into a groove of the E3 RING domain (Zheng et al., 2000). We used the c-Cbl RING domain to construct a homology model of the Rad5 RING domain bound to Mms2/Ubc13 by assuming that Ubc13 binds to the Rad5 RING domain in a manner similar to the c-Cbl/UbcH7 interaction (Figure 6). The model suggests that interaction of the Mms2/Ubc13 and UEV1a/Ubc13 complexes with their RING partner proteins Rad5 (Ulrich and Jentsch, 2000) and Traf6 (Deng et al., 2000) will not occlude any interactions with either donor or acceptor ubiquitin. The binding of RING domain proteins to UEV/Ubc13 complexes should therefore not alter linkage specificity in chain assembly, in agreement with results obtained in biochemical studies of Traf6 and the UEV1a/

Table 1. Statistics from the Crystallographic Analysis

| Crystal | Ubc13 Alone | Mms2/Ubc13 Complex |
|---|---|---|
| X-ray source | RAXIS IV | NSLS X4A |
| Temperature | 298K | 100K |
| Resolution (Å) | 2.0 | 1.6 |
| Observations | 55,421 | 185,078 |
| Unique Reflections | 17,787 | 36,126 |
| Completeness (%) | 93.6 (83.2) | 98.8 (97.9) |
| Overall $I/\sigma(I)$ | 27.8 (4.4) | 23.0 (3.8) |
| $R_{sym}$ (%) | 5.3 (22.3) | 6.7 (35.9) |
| Mosaicity | 0.33 | 0.78 |
| **Refinement Statistics** | | |
| Total atoms | 2,529 | 2,535 |
| R factor (%) | 18.8 | 20.3 |
| $R_{free}$ (%) | 26.1 | 23.9 |
| Rmsd bonds (Å) | 0.0084 | 0.0097 |
| Rmsd angles (°) | 1.53 | 1.60 |

$R_{sym} = \Sigma_h\Sigma_i|I_{h,i} - I_h|/\Sigma_h\Sigma_i I_{h,i}$ for the intensity ($I$) of i observations of reflection $h$.
R factor $= \Sigma||F_{obs}| - |F_{calc}||/\Sigma|F_{obs}|$, where $F_{obs}$ and $F_{calc}$ are the observed and calculated structure factors, respectively. $R_{free}$ = R factor calculated using 5% of the reflection data chosen randomly and omitted from the start of refinement. Statistics for the outer shell are in parentheses. Rmsd: root mean square deviations from ideal geometry.

Ubc13 complex (Deng et al., 2000). Although numerous examples of RING E3 proteins are known (Joazeiro and Weissman, 2000), RING domain proteins can also be substrates of modification by ubiquitin (Buschmann et al., 2000). It remains to be determined whether Traf6 and Rad5 are E3 enzymes or substrates of the respective UEV/Ubc13 complexes.

## Conclusions

Linkage specificity in ubiquitin chain assembly allows for the generation of a diverse set of polyubiquitin chains whose cellular functions are distinct. The Mms2/Ubc13 heterodimer exclusively catalyzes the assembly of K63 polyubiquitin chains, and this catalysis is dependent on the binding of Mms2 to Ubc13; Mms2 or Ubc13 alone will not assemble chains of any linkage type. The asymmetric Mms2/Ubc13 complex is stabilized by a combination of electrostatic and hydrophobic contacts that are, in part, mediated by residues of Mms2—notably Asn7 and Phe8—that are unique to UEVs (Figure 1C). Residues making up the interface of the yeast Mms2/Ubc13 complex are highly conserved in human UEV1a and Ubc13. Thus, it appears highly likely that the human UEV1a/Ubc13 complex, which assembles K63-chains important in IKK activation, shares a very similar architecture to the Mms2/Ubc13 complex. Consistent with this idea, the two complexes share striking biochemical similarities (Deng et al., 2000; Hofmann and Pickart, 1999) and the overexpression of human UEV1a complements the DNA repair defect of yeast deleted for the *MMS2* gene (Thomson et al., 1998; Xiao et al., 1998). We have demonstrated the importance, in vivo, of heterodimer formation by our finding that mutations which inhibit Mms2/Ubc13 complex formation produce a defect in DNA repair equivalent to a null mutation in either gene.

A striking feature of the UbcH7/c-Cbl and UbcH7/E6-AP E2-E3 structures is that while the E3 is required for assembly of polyubiquitin chains on the substrate, the E3 does not provide any residues for chemical catalysis (Huang et al., 1999; Zheng et al., 2000). Indeed, the closest approach of any E3 residue to the E2 active site thiol is ~15 Å. In view of this unexpected feature, it has been suggested that catalysis reflects principally an induced proximity of substrate (bound to the E3) and ubiquitin (bound to the E2). The Mms2/Ubc13 complex follows this trend, as no Mms2-derived side chain approaches Cys87 closely enough to be a credible candidate for a chemical catalyst. Rather, Mms2 provides a platform that binds the acceptor ubiquitin in an orientation that allows only Lys63, and not Lys48, to approach the active site. These results show for the first time how a simple molecular scaffold can provide the high degree of specificity necessary in ubiquitin chain assembly and suggests a general model for how binding of accessory proteins to E2 enzymes can guide the conjugation of ubiquitin with substrates.

## Experimental Procedures

### Plasmids and Antibodies

Plasmid pET16b-ScMms2 has been described (Hofmann and Pickart, 1999). In pGEX-ScUbc13, the yeast Ubc13 coding sequence was cloned downstream of the thrombin cleavage site of pGEX-4T2 (Amersham-Pharmacia). To create $pH_{10}$-Mms2, the $His_{10}$-Mms2 sequence under the control of the endogenous *MMS2* promoter was cloned into a *URA3*-marked version of the centromeric vector pRS316. To create pUbc13-$HA_3$, the Ubc13 sequence (with its intron) was cloned downstream of the endogenous *UBC13* promoter in a centromeric *LEU2*-marked vector specifying a C-terminal triple-hemaglutinin (HA) tag (gift of O. Kershner). Antibodies against the polyHis and HA tags were purchased from Santa Cruz. Mutations were introduced by whole-plasmid PCR using appropriate mutagenic primers via the Quick-Change mutagenesis kit (Stratagene). All mutations were verified by DNA sequencing.

### Protein Purification

$His_{10}$Mms2 was expressed in BL21pJY2 cells as described (Hofmann and Pickart, 1999; You et al., 1999), purified on nickel beads under denaturing conditions (4 M Urea, 50 mM HEPES [pH 8.0], 0.5 M NaCl, 5% gylcerol, 1 mM β-mercaptoethanol, 1 μM AEBSF), and refolded by dialysis. Ubc13 was expressed using pGEX-ScUbc13 and released from the GST-Ubc13 fusion protein (immobilized on GSH beads) by thrombin cleavage. The resulting protein initiates with Ala2. For crystallography, the $His_{10}$ tag was removed from Mms2 with Factor Xa, the Mms2 and Ubc13 were mixed in a 1:1 ratio, and the complex was purified on a MonoQ column in buffer containing 5% glycerol. The reconstituted complex was active in K63-chain synthesis prior to crystallization (data not shown). For biochemical assays, mutant and wild-type Mms2 and Ubc13 proteins were purified separately and mixed in the assay. In the case of D81R-Ubc13, the GST fusion was eluted with reduced glutathione prior to cleavage with thrombin, then mixed with $His_{10}$Mms2. The complex was then purified by nickel bead chromatography. The intact tagged version of Mms2 was used for biochemical studies. The tagged protein is fully functional in DNA repair in vivo (R.H. and C.P., unpublished data).

### Crystallization and Data Collection

Purified Ubc13 (12 mg/ml) was dialyzed into 10 mM HEPES (pH 8.0), 10 mM NaCl, 5 mM DTT. Crystals were grown using the hanging drop vapor diffusion method at 20°C by mixing equal volumes of protein with a reservoir solution containing 30% PEG5000-MME, 200 mM ammonium sulfate, 50 mM MES (pH 6.5), 2 mM DTT. Data were collected at room temperature at the Cu-Kα edge using a RAXIS-IV image plate detector equipped with double-focusing mirrors. Crystals formed in space group $P2_1$ with unit cell dimensions a = 26.0 Å, b = 129.4 Å, c = 42.9 Å, β = 96.4° and contained two molecules in the asymmetric unit. The Mms2/Ubc13 complex was dialyzed into buffer containing 10 mM HEPES (pH 8.0), 10 mM NaCl, 1 mM EDTA, 5 mM b-mercaptoethanol, 5% glycerol and concentrated to ~10 mg/ml by ultrafiltration. Crystals were obtained by the hanging drop vapor diffusion method at 20°C by mixing the complex with an equal volume of reservoir solution containing 35% PEG 1000, 50 mM Tris (pH 7.5), 2 mM DTT. The crystals formed in space group $P2_1$ with unit cell dimensions a = 53.0 Å, b = 63.6 Å, c = 43.1 Å, β = 105.8° and contained one complex in the asymmetric unit. Crystals were frozen at 100 K using reservoir solution supplemented with 20% glycerol as the cryoprotectant. Diffraction data were collected at beamline X4A of NSLS (l = 0.912 Å) and processed with DENZO and SCALEPACK (Otwinowski and Minor, 1997). Crystallographic statistics are shown in Table 1.

### Structure Determination and Refinement

The structure of Ubc13 alone was solved by molecular replacement with the program MOLREP (Collaborative Computational Project, 1994) using the structure of Ubc4 (Protein Data Bank Id code 1QCQ) (Cook et al., 1993) as the search model. The structure was built with the model building program XFIT (McRee, 1999). The model was refined using CNS (Brunger et al., 1998) and contains residues (3–28, 30–150) from molecule A, residues (3–29, 31–149) from molecule B, and 190 water molecules.

The structure of the Mms2/Ubc13 complex was solved by first determining the position of Ubc13 using MOLREP (Vagin and Teplyakov, 1997) using Ubc13 as the search model. A molecular replacement solution was also obtained for residues 38–77 of Mms2, using Ubc13 32–71 as the search model, and phases were then calculated for the entire complex. ARP/wARP (Lamzin and Wilson, 1993) was

used for initial model building of Mms2 and further model building was done using XFIT (McRee, 1999). The model was refined using CNS (Brunger et al., 1998) and contains Ubc13 residues 2–152, Mms2 residues (2–19, 24–137), and 276 water molecules. Alternative conformations are included for Ubc13 residues Val69, Leu88, Trp129 and Mms2 residues Cys26, Ile57, Ile81, and Arg129. Mms2 residues 20–23 are disordered.

### Chain Assembly Assays

Two assays were used, with both carried out under conditions that yield diubiquitin as the sole product in order to facilitate quantitative rate measurements. In the first assay (Hofmann and Pickart, 1999), a high concentration of D77-ubiquitin (117 mM) served as acceptor while a low concentration of $^{125}$I-ubiquitin (5 mM) served as donor. Incubations (conditions as in Hofmann and Pickart, 1999) containing 0.2 mM each of Mms2 and Ubc13 (and 0.1 mM E1) were sampled in the linear rate period and resolved by SDS-PAGE prior to counting the excised $^{125}$I-diubiquitin band. Studies of competition by K63-tetraubiquitin employed the same assay, but with a reduced concentration of D77-ubiquitin (25 mM). In the second assay, D77-ubiquitin and K63R-ubiquitin (117 mM each) served as acceptor and donor, respectively, in incubations containing 2 mM each of Mms2 and Ubc13 (with 0.1 mM E1). The diubiquitin product was visualized by SDS-PAGE and Coomassie staining. Pulse-chase assays to measure the intrinsic rate of ubiquitin-ubiquitin conjugation were carried out essentially as described previously (Chen et al., 1991). The pulse contained 4 mM each of Mms2 and Ubc13 and 2 mM of $^{125}$I-ubiquitin; the chase was initiated by adding 117 mM wild-type ubiquitin as acceptor. The method for assembly of K63-tetraubiquitin was modified from that employed previously to make K48-tetraubiquitin (Piotrowski et al., 1997) and will be described in detail elsewhere (R.H. and C.P., unpublished data).

### Direct Assay of Mms2/Ubc13 Binding

In most cases, $His_{10}$Mms2 was mixed with a slight excess of Ubc13 and then immobilized on nickel beads and then mixed with Ubc13 in a buffer containing 50 mM Tris (pH 8), 0.2 mg/ml BSA. The immobilized complex was washed with this buffer and then eluted with increasing concentrations of NaCl in the same buffer. For Mms2-F8A and its control, a slight excess of Mms2 was immobilized first and then mixed with wild-type Ubc13 prior to proceeding as described above.

### UV Sensitivity Measurements

The *MMS2* and *UBC13* genes were deleted from strain SUB62 (Finley et al., 1994) using *URA3*-marked disruption plasmids followed by selection against the marker using 5-fluoorotic acid (Alani et al., 1987; Hofmann and Pickart, 1999). The resulting double null strain was transformed with $pH_{10}$-Mms2 and pUbc13-$HA_3$ (above) that specified either wild-type or mutant versions of the respective proteins (Mms2-F8A or Ubc13-E55A). The resulting strains were grown on selective medium and tested for UV sensitivity as described (Hofmann and Pickart, 1999).

### Acknowledgments

We thank A. Raguraj and B. So for technical assistance; C. Garvie, N. LaRonde-LeBlanc, J. Avalos, and A. Key for help with data collection; C. Garvie and R. Campbell for crystallographic advice; and C. Ogata and R. Abramowitz of NSLS beamline X4A for technical support. This work was supported by the Howard Hughes Medical Institute (C.W.), the NIH (GM60372, C.P.), and by a training grant from NIEHS.

Received April 4, 2001; revised May 23, 2001.

### References

Alani, E., Cao, L., and Kleckner, N. (1987). A method for gene disruption that allows repeated use of *URA3* selection in the construction of multiply disrupted yeast strains. Genetics *116*, 541–545.

Beal, R., Deveraux, Q., Xia, G., Rechsteiner, M., and Pickart, C. (1996). Surface hydrophobic residues of multiubiquitin chains essential for proteolytic targeting. Proc. Natl. Acad. Sci. USA *93*, 861–866.

Broomfield, S., Chow, B.L., and Xiao, W. (1998). *MMS2*, encoding a ubiquitin-conjugating-enzyme-like protein, is a member of the yeast error-free postreplication repair pathway. Proc. Natl. Acad. Sci. USA *95*, 5678–5683.

Brunger, A.T., Adams, P.D., Clore, G.M., DeLano, W.L., Gros, P., Grosse-Kunstleve, R.W., Jiang, J.S., Kuszewski, J., Nilges, M., Pannu, N.S., et al. (1998). Crystallography & NMR system: A new software suite for macromolecular structure determination. Acta. Crystallogr. D Biol. Crystallogr. *54*, 905–921.

Brusky, J., Zhu, Y., and Xiao, W. (2000). *UBC13*, a DNA-damage-inducible gene, is a member of the error-free postreplication repair pathway in Saccharomyces cerevisiae. Curr. Genet. *37*, 168–174.

Buschmann, T., Fuchs, S.Y., Lee, C.G., Pan, Z.Q., and Ronai, Z. (2000). SUMO-1 modification of Mdm2 prevents its self-ubiquitination and increases Mdm2 ability to ubiquitinate p53. Cell *101*, 753–762.

Chau, V., Tobias, J.W., Bachmair, A., Marriott, D., Ecker, D.J., Gonda, D.K., and Varshavsky, A. (1989). A multiubiquitin chain is confined to specific lysine in a targeted short-lived protein. Science *243*, 1576–1583.

Chen, Z.J., Niles, E.G., and Pickart, C.M. (1991). Isolation of a cDNA encoding a mammalian multiubiquitinating enzyme ($E2_{25K}$) and overexpression of the functional enzyme in Escherichia coli. J. Biol. Chem. *266*, 15698–15704.

Chen, Z.J., Parent, L., and Maniatis, T. (1996). Site-specific phosphorylation of IκBα by a novel ubiquitination-dependent protein kinase activity. Cell *84*, 853–862.

Collaborative Computational Project, N. (1994). CCP4. Acta. Cryst. *D50*, 760–763.

Cook, W.J., Jeffrey, L.C., Sullivan, M.L., and Vierstra, R.D. (1992). Three-dimensional structure of a ubiquitin-conjugating enzyme (E2). J. Biol. Chem. *267*, 15116–15121.

Cook, W.J., Jeffrey, L.C., Xu, Y., and Chau, V. (1993). Tertiary structures of class I ubiquitin-conjugating enzymes are highly conserved: crystal structure of yeast Ubc4. Biochemistry *32*, 13809–13817.

Deng, L., Wang, C., Spencer, E., Yang, L., Braun, A., You, J., Slaughter, C., Pickart, C., and Chen, Z.J. (2000). Activation of the IκB kinase complex by TRAF6 requires a dimeric ubiquitin-conjugating enzyme complex and a unique polyubiquitin chain. Cell *103*, 351–361.

Finley, D., Sadis, S., Monia, B.P., Boucher, P., Ecker, D.J., Crooke, S.T., and Chau, V. (1994). Inhibition of proteolysis and cell cycle progression in a multiubiquitination-deficient yeast mutant. Mol. Cell. Biol. *14*, 5501–5509.

Gabb, H.A., Jackson, R.M., and Sternberg, M.J. (1997). Modelling protein docking using shape complementarity, electrostatics and biochemical information. J. Mol. Biol. *272*, 106–120.

Galan, J., and Haguenauer-Tsapis, R. (1997). Ubiquitin Lys63 is involved in ubiquitination of a yeast plasma membrane protein. EMBO J. *16*, 5847–5854.

Hershko, A., and Ciechanover, A. (1998). The ubiquitin system. Annu. Rev. Biochem. *67*, 425–479.

Hicke, L. (1999). Gettin' down with ubiquitin: turning off cell-surface receptors, transporters and channels. Trends Cell Biol. *9*, 107–112.

Hofmann, R.M., and Pickart, C.M. (1999). Noncanonical *MMS2*-encoded ubiquitin-conjugating enzyme functions in assembly of novel polyubiquitin chains for DNA repair. Cell *96*, 645–653.

Huang, L., Kinnucan, E., Wang, G., Beaudenon, S., Howley, P.M., Huibregtse, J.M., and Pavletich, N.P. (1999). Structure of an E6AP-UbcH7 complex: insights into ubiquitination by the E2–E3 enzyme cascade. Science *286*, 1321–1326.

Humphrey, W., Dalke, A., and Schulten, K. (1996). VMD—visual molecular dynamics. J. Mol. Graph. *14*, 33–38.

Jentsch, S., McGrath, J.P., and Varshavsky, A. (1987). The yeast DNA repair gene *RAD6* encodes a ubiquitin-conjugating enzyme. Nature *329*, 131–134.

Jiang, F., and Basavappa, R. (1999). Crystal structure of the cyclin-

specific ubiquitin-conjugating enzyme from clam, E2-C, at 2.0 Å resolution. Biochemistry *38*, 6471–6478.

Joazeiro, C.A., and Weissman, A.M. (2000). RING finger proteins: mediators of ubiquitin ligase activity. Cell *102*, 549–552.

Joazeiro, C.A., Wing, S.S., Huang, H., Leverson, J.D., Hunter, T., and Liu, Y.C. (1999). The tyrosine kinase negative regulator c-Cbl as a RING-type, E2-dependent ubiquitin-protein ligase. Science *296*, 309–312.

Johnson, R.E., Henderson, S.T., Petes, T.D., Prakash, S., Bankmann, M., and Prakash, L. (1992). Saccharomyces cerevisiae *RAD5*-encoded DNA repair protein contains DNA helicase and zinc-binding sequence motifs and affects the stability of simple repetitive sequences in the genome. Mol. Cell. Biol. *12*, 3807–3818.

Kaiser, P., Flick, K., Wittenberg, C., and Reed, S.I. (2000). Regulation of transcription by ubiquitination without proteolysis: Cdc34/SCF(Met30)-mediated inactivation of the transcription factor Met4. Cell *102*, 303–314.

Koegl, M., Hoppe, T., Schlenker, S., Ulrich, H.D., Mayer, T.U., and Jentsch, S. (1999). A novel ubiquitination factor, E4, is involved in multiubiquitin chain assembly. Cell *96*, 635–644.

Koepp, D.M., Harper, J.W., and Elledge, S.J. (1999). How the cyclin became a cyclin: regulated proteolysis in the cell cycle. Cell *97*, 431–434.

Koonin, E.V., and Abagyan, R.A. (1997). TSG101 may be the prototype of a class of dominant negative ubiquitin regulators. Nat. Genet. *16*, 330–331.

Lamzin, V., and Wilson, K. (1993). Automated refinement of protein models. Acta Cryst. *D49*, 129–147.

McRee, D.E. (1999). XtalView/Xfit—a versatile program for manipulating atomic coordinates and electron density. J. Struct. Biol. *125*, 156–165.

Merritt, E. and Bacon, D. (1997). Raster3D: photorealistic molecular graphics. Methods Enzymol. *277*, 505–524.

Miura, T., Klaus, W., Gsell, B., Miyamoto, C., and Senn, H. (1999). Characterization of the binding interface between ubiquitin and class I human ubiquitin-conjugating enzyme 2b by multidimensional heteronuclear NMR spectroscopy in solution. J. Mol. Biol. *290*, 213–228.

Otwinowski, Z., and Minor, W. (1997). Processing of X-ray diffraction data collected in oscillation mode. Methods Enzymol. *276*, 307–326.

Pickart, C.M. (2000). Ubiquitin in chains. Trends Biochem. Sci. *25*, 544–548.

Piotrowski, J., Beal, R., Hoffman, L., Wilkinson, K.D., Cohen, R.E., and Pickart, C.M. (1997). Inhibition of the 26 S proteasome by polyubiquitin chains synthesized to have defined lengths. J. Biol. Chem. *272*, 23712–23721.

Rock, K.L., and Goldberg, A.L. (1999). Degradation of cell proteins and the generation of MHC class I-presented peptides. Annu. Rev. Immunol. *17*, 739–779.

Sancho, E., Vila, M.R., Sanchez-Pulido, L., Lozano, J.J., Paciucci, R., Nadal, M., Fox, M., Harvey, C., Bercovich, B., Loukili, N., et al. (1998). Role of UEV-1, an inactive variant of the E2 ubiquitin-conjugating enzymes, in vitro differentiation and cell cycle behavior of HT-29–M6 intestinal mucosecretory cells. Mol. Cell. Biol. *18*, 576–589.

Spence, J., Gali, R.R., Dittmar, G., Sherman, F., Karin, M., and Finley, D. (2000). Cell cycle-regulated modification of the ribosome by a variant multiubiquitin chain. Cell *102*, 67–76.

Spence, J., Sadis, S., Haas, A.L., and Finley, D. (1995). A ubiquitin mutant with specific defects in DNA repair and multiubiquitination. Mol. Cell. Biol. *15*, 1265–1273.

Thomson, T.M., Khalid, H., Lozano, J.J., Sancho, E., and Arino, J. (1998). Role of UEV-1A, a homologue of the tumor suppressor protein TSG101, in protection from DNA damage. FEBS Lett. *423*, 49–52.

Ulrich, H.D., and Jentsch, S. (2000). Two RING finger proteins mediate cooperation between ubiquitin-conjugating enzymes in DNA repair. EMBO J. *19*, 3388–3397.

Vagin, A., and Teplyakov, A. (1997). MOLREP: an automated program for molecular replacement. J. Appl. Cryst. *30*, 1022–1025.

Worthylake, D.K., Prakash, S., Prakash, L., and Hill, C.P. (1998). Crystal structure of the Saccharomyces cerevisiae ubiquitin-conjugating enzyme Rad6 at 2.6 A resolution. J. Biol. Chem. *273*, 6271–6276.

Xiao, W., Lin, S.L., Broomfield, S., Chow, B.L., and Wei, Y.F. (1998). The products of the yeast MMS2 and two human homologs (hMMS2 and CROC-1) define a structurally and functionally conserved Ubc-like protein family. Nucleic Acids Res. *26*, 3908–3914.

Xiao, W., Chow, B.L., Broomfield, S., and Hanna, M. (2000). The Saccharomyces cerevisiae RAD6 group is composed of an error-prone and two error-free postreplication repair pathways. Genetics *155*, 1633–1641.

You, J., Cohen, R.E., and Pickart, C.M. (1999). Construct for high-level expression and low misincorporation of lysine for arginine during expression of pET-encoded eukaryotic proteins in Escherichia coli. Biotechniques *27*, 950–954.

Zheng, N., Wang, P., Jeffrey, P.D., and Pavletich, N.P. (2000). Structure of a c-Cbl-UbcH7 complex: RING domain function in ubiquitin-protein ligases. Cell *102*, 533–539.

**Accession Numbers**

The coordinates for the Ubc13 and Mms2/Ubc13 structures have been deposited in the Protein Data Bank with ID codes 1JBB and 1JAT, respectively.